10 min, rinsed with PBS. Formalin-fixed tissue sections were also used for immunostaining. A rabbit polyclonal anti-humanin antibody was synthesized and purified on an affinity column and dissolved into PBS (0.9% NaCl, 0.02M phosphate buffer, pH7.0). The IgG concentration was analyzed using the Protein Assay kit (Bio-Rad). Immunostaining was performed as previously described.(22,23) Briefly, cells and sections were fixed with 4% formaldehyde in PBS. Following a rinse with PBS, membrane perforation treatment was performed with 95% ethanol/ 5% acetic acid for 10 minutes. After washing with PBS and blocking by incubation with 1% BSA, excess BSA was then removed and the cells were incubated with anti-humanin antibodies overnight at 4°C. After rinsing, Alexa Fluor 488 goat anti-rabbit IgG (Molecular Probes, Inc.) was applied as a secondary antibody for 60 min. Immunofluorescence was detected using a CSU-10 confocal laser scanning unit (Yokogawa Electric Co.), coupled to an IX90 inverted microscope with UPlanAPOX20 objective lens (Olympus Potical Co.), and C5810-01 color chilled 3CCD camera(Hamamatsu Photonics, K.K.). For double staining, anti-humanin antibody and anti-HSP60 antibody (Santa Cruz Biochemistry Inc.) were used as first antibodies, while Alexa fluor 568 goat anti-rabbit IgG and Alexa Fluor 488 donkey anti-goat IgG (Molecular Prob Inc.) were used as a second antibodies.

Western blot analysis.

Tissues were homogenized and lysed in a buffer consisting of 150 mM NaCl, 50mM Tris HCl, pH7.5, 0.5% Nonidet 40, 50mM NaF, 1mM Na_3VO_4, 1mM PMSF and 1% aprotinin at 4 °C for 30 min. Cell lysates were cleared of cell debris by centrifugation at 14,000g for 30 min.

Twenty μg of protein were subjected to sodium dodecylsulfate-polyacrylamide gel electrophoresis (SDS-PAGE) on a PAG mini Daiichi 15/25 gel (Daiichi Pure Chemical Co.). The gel electrophoresis was performed under non-reducing conditions. The proteins were then blotted on a nitrocellulose blotting membrane (Osmonics Inc.). Nitrocellulose membranes were blocked with 5 % BSA, followed by washing with PBS-Tween 20 and incubated with rabbit anti-humanin antibody at 4 °C overnight. After intensive washing, membranes were incubated with horseradish peroxidase-linked goat anti-rabbit IgG, followed by detection with ECL reagents (Biotechs).

Electron Microscope and Colloidal-Gold immunocytochemistry.

Synovial cells from diffuse type PVNS were gathered in the same manner for light microscopy, and fixed in 3% glutaraldehyde in 0.1M phosphate buffer (pH 7.4) at 4°C over night. The specimens were postfixed in 1% OsO_4 in 0.1M phosphate buffer (pH 7.4) overnight at 4°C, rinsed three times (10 min each) in 10% saccharose, and stained *en bloc* in 3% aqueous uranyl acetate for 1 hr at room temperature. Samples were then dehydrated in an ascending series of ethanol concentrations, replaced by proplene oxide and embedded in epoxy resin. Ultrathin sections (100 nm) were cut, stained with uranyl acetate and lead citrate, and observed using an electron microscope (Hitachi H-7000).

For electron microscopic immunocytochemistry, cells were fixed in 0.2% glutaraldehyde and 4% paraformaldehyde mixture in 0.1 M phosphate buffer (pH 7.4) at 4°C overnight. The samples were embedded into Lowicryl K4M and ultrathin sections (100nm) were used for

incubation with anti-humanin antibody overnight. Incubation with the biotinylated secondary antibody was performed at room temperature for 1 hour, and after washing with PBS and distilled water, incubation with Colloidal-gold streptavidin was performed for 1 hour. After the sections were rinsed and dried, they were stained with uranyl acetate and lead citrate, and electron microscope was performed as described above.

RESULTS

Identification of highly expressed genes in PVNS

A total of 2956 clones selected by subtraction cloning were further examined by Southern colony hybridization. The sequencing was performed on genes expressed in PVNS at three-times greater frequency than those in RA. Sixty eight of the highly expressed genes were identical to 17 known genes. Two genes were identical to genes encoding two hypothetical proteins. In Table 1, these genes were classified into 7 groups according to their functions and whether they were transcribed in mitochondria. Interestingly, genes encoded in the region of 16S rRNA and 12S rRNA were expressed with high frequencies. Furthermore, we detected various forms of 16S rRNA with poly A tail end, as shown in Fig. 1. There was no 12S rRNA with poly A tail among these genes. The cDNA with polyA tail (16SrRNA•3229: Type 9 in Fig. 1) was identical to the humanin gene.

Northern blot analysis was performed using mRNA of synovial cells from PVNS, RA and OA patients. Humanin genes were strongly expressed in diffuse type PVNS, but were barely

detectable in nodular type PVNS, RA, or OA (Fig. 2). However, other genes encoded by mitochondria were not increased as assessed by semiquantitative RT-PCR, suggesting that ribosomal genes were selectively expressed in mitochondrial genes in PVNS (Fig. 3). This is the first report of the expression of humanin gene in synovial cells.

Expression of the humanin peptide in PVNS

Next, the expression of humanin peptide was identified using synovial cell lysates from diffuse type PVNS and anti-humanin polyclonal anti-body (Fig. 4). Immunohistochemical analysis showed that most of the positive cells were distributed in the deep layer (Fig. 5). This positive staining was thoroughly suppressed by blocking the primary antibody with synthesized antigen peptide (data not shown).

Although it has been suggested that the humanin peptide is expressed by cells in the deep layer of PVNS, little is known about the intracellular localization of this peptide. In further examinations, we detected intracellular humanin peptide in synovial cells from diffuse type PVNS. The humanin peptide was stained with red color which localized in the cytoplasm of the synovial cells (Fig.6-b) but not in the nucleus. Mitochondria was stained with green colar using anti-heat shock protein 60, which is mitochondrial specific chaperonin (Fig. 6-c). Double staining with anti-humanin antibody and anti-heat shock protein 60 (yellow color) demonstrated that humanin was expressed mainly in mitochondria (Fig.6-d).

Electron microscopic observation of synovial cells from diffuse type PVNS revealed that most of the iron deposits were included within the siderosome as described previously.(16,17) However, some electron dense iron deposits were observed within mitochondria (Fig.7-a). Interestingly, mitochondrial membrane debris with electron dense iron deposits were observed within the siderosome which was characterized as an autophagosome (Fig.7-a). On the other hand, some normal mitochondria were scattered throughout the cytoplasm (Fig7-b). Electron dense iron deposits within the siderosome were observed by electron microscopic immunohistochemistry (Fig. 8). In some siderosomes, particles of colloidal-gold were precipitated to the debris adjacent to electron dense iron (Fig. 8-a). These results suggest that humanin exists in mitochondria not only in the cytoplasm but also in the siderosome after being phagocytosed.

DISCUSSION

Genes with enhanced expression in synovial cells from PVNS were grouped according to their functions and the transcription in mitochondria as listed in Table 1. It is likely that many of the listed genes may be involved in the pathogenesis of PVNS according to their characterized functions. Interestingly, genes encoded in the regions of 16S rRNA and 12S rRNA were expressed with high frequencies. Previous reports pointed out the presence of polyadenylated transcripts of the 16S rRNA gene that were different from the 16S rRNA. (24,25,26) These poly A sequences are considered to be due to active metabolism of mitochondria in cancer cells, since the increased expression of the 16S rRNA genes was found

only in malignancies. (19,27) These facts suggest that the genes encoded in the region of rRNA from PVNS reflect the neoplastic nature of this disease. In fact, for PVNS, especially the diffuse type, the neoplastic hypothesis is supported by the demonstration of aneuploid DNA content and the existence of cytogenetic aberration, as well as the capacity of these lesions for autonomous growth and the potential for recurrence. (13,14)

It is intriguing to examine whether these mitochondrial genes for 16S rRNA are virtually translated and act as functional peptides. In this regard, humanin is a polypeptide described as a rescue factor abolishing neural cell apoptosis. This peptide protects neural cells of the F11 line from death induced by the expression of mutated genes, causing early-onset familiar Alzheimer's disease.(28) Additionally, it was reported that humanin protects CN-procaspase-3 from amyloid precursor protein-induced cleavage, thereby preventing apoptosis.(29,30,31) More recently, Guo et al. (20) also described the anti-apoptotic mechanism of this peptide through interference with Bax activation. In this study, we proved that the humanin peptide, encoded in the mitochondrial genome, was selectively expressed in the mitochondria and within the siderosome in the diffuse type PVNS synovial cells. It is well established that damaged and functionally disabled mitochondria may be autophagocytosed by lysosomes to prevent continuous oxidative damage, as shown in the degenerating mitochondria within the siderosome in our electron microscopic study. (32,33) This evidence suggests that humanin is translated in mitochondria, causing survival of this organelle under the condition of excessive iron deposition.

In fact, extreme iron deposition is one of the most characteristic pathological features in PVNS. (2,7,8) This deposit is derived from the breakdown of erythrocytes that are phagocytosed after repeated bleeding into the joint space. (16,34,35) Under the condition of iron excess, some of the iron is shunted into hemosiderin and stored in the cytoplasm. (36) It is well described that reactive oxygen species are generated by excessive iron-induced cell apoptosis, which is one important mechanism implicated in the mitochondrial death pathway. (36,37,38,39,40) This mechanism may involve the capacity of excessive iron deposits to stimulate lipid peroxidation, thereby disrupting lysosomal membranes and releasing tissue destructive hydrolytic enzymes.(41,42) In regard to PVNS, as shown in our subtraction cloning, the iron deposits are known to be associated with large quantities of ferritin. Nevertheless, homogeneous synovial cells with small, rounded siderosomes in the deep layer of synovium, which present predominantly in diffuse type PVNS, were reported to have minimum tissue damage adjacent to the iron deposits.(43) Morris et al. (43) reported that electron dense iron deposits were associated with mitochondrial destruction in haemophilic synovitis but much less in PVNS. Several explanations were described for this lack of mitochondrial damage in previous reports, such as transitional function during inflammation, or the failure of the apoferritin response.(31,43) However, there were no facts to explain this pathology.

The alternative intriguing explanation about this pathogenesis of PVNS is that a mitochondrial abnormality exists primarily in PVNS independent of the precipitation of hemosiderin. In that case, the overload of iron deposits in the cytoplasm and mitochondria could induce free radicals.

However, abnormal mitochondria would be responsible for supplying a key reactant, humanin, to prevent oxidative damage until they are autophagocytosed within siderosome, resulting in cell survival. In accordance with this view, analysis of isolated cells has enabled us to describe here for the first time the feature of hemosiderin-containing mitochondria, which was autophagocytosed and degenerating within the siderosome, in addition to many mitochondria without hemosiderin scattered around the cytoplasm.

Taken together, our findings lead us to a simple interpretation that the possible function of humanin located within the mitochondria in PVNS synovial cells may be to serve as a rescue factor from excessive iron damage and consequent organelle breakdown in the cytoplasm and cell death. However, Hashimoto et al. (19,23) have shown that cell death is only supported by the secreted humanin peptide, and the function of the peptide located intracellularly is still unclear. Although future studies are required to investigate the function of humanin within the cytoplasm, our data suggest that humanin is involved in the iron depositing pathology of PVNS. In conclusion, our results suggest that the humanin peptide is highly expressed in the synovial cells from diffuse type PVNS and may be involved in the pathology of PVNS.

ACKNOWLEDGEMENT

The authors thank A.Tsuchiya MD and S.Tsuyama MD for their professional advice.

REFFERENCES

1. Jaffe HL, Lightenstein L,Sutro CJ: Pigmented villonodular synivitis, bursitis and tenosynovitis. Arch Pathol 31:731-765,1941

2. Dorwart RH, Genant HK, Johnston WH, et al: Pigmented villonodular synovitis of synovial joints:Clinical, pathologic, and radiologic features. Am J Roentgenlo 143:877-885,1984

3. Darling JM, Glimcher LH, Shortkroff S, Albano B, Gravallese EM.:Expression of metalloproteinases in pigmented villonodular synovitis. Hum Pathol 25:825-830,1994

4. Gehweiler JA, Wilson JW: Diffuse biarticular pigmented villonodular synovitis. Radiology 93:845-851,1969

5. Crosby EM, Inglis A, Bullough PG: Mulitple joint involvement with pigmented villonodular synovitis. Radiology122:671-672,1977

6. Wagner ML, Spjut HJ, Dutton RV, Glassman AL, Askew JB: Polyarticular pigmented villonudular synovitis. AJR 136:821-823,1981

7. Byers PD, Cotton RE, Deacon OW, et al:The diagnosis and treatment of pigmented villonodular synovitis. J Bone Joint Surg[Br] 50:290-305,1968

8. Laszlo Jozsa: Immunohistochemical characterization of pigmented villonodular synovitis. Zentralbl Pathol 138: 119-123,1992

9. O'Connell JX, Fanburg JC, Rosenberg AE: Giant cell tumor of tendon sheath and pigmented villonodular synovitis. Immunophenotype suggests a synovial cell origin. Human Pathol 26:771-5,1995

10. Darling JM, Goldring SR, Harada Y, et al: Multinuclear cells in pigmented villonodular

synovitis and and giant cell tumor of tendon sheath express features of osteoclasts. Am J Pathol 150: 1383-92,1997

11. Young JM, Hudacek AG: Experimental production of pigmented villonodular synivitis in dogs. Am J Pathol 30:799-811,1954

12. Sigh R, Grewal DS, Chakravarti RN: Experimental production of pigmented villonodular synovitis in the knee and ankle joints of rhesus monkey. J Path 98:137-142,1969

13. Somerhausen NSA, Flrcher CDM: Diffuse-tupe giant cell tumor. Clinicopathologic and immunohistochemical analysis of 50 cases with extraarticular disease. Am J Surg Pathol 24:479-492,2000

14. Abdul-Karim FW, El-Naggar AK. Joyce MJ, Makley JT, Carter JR. Diffuse and localized tenosynovial giant tumor and pigmented villonodular synovitis: a clinicopathological and flow cytometric DNA analysis. Hum Pathol 23:729-35,1992

15. Fletcher JA, Henkle C, Atkins L, Rosenberg AE, Morton C. Trisomy 5 and trisomy 7 are nonrandom aberrations in pigmented villonodular synovitis: confirmation of trisomy 7 in uncultured cells. Genes chromosomes cancer 4:264-266,1992

16. Schumacher HR, Lotke P, Athreya B, Rothfuss S. Pigmented villonodular synovitis:light and electron microscopic studies. Semin Arthrits Rheum 12:32-43,1982

17. Ghadially FN, Lalonde J-M A, Dick CE. Ultrastructure of pigmented villonodular synovitis. J Path.127:19-27,1978

18. Wyllie JC. Stromal cell reaction of pigmented villonodular synovitis: an electron

microscopic study. Arthritis Rheum. 12(3):205-214,1969

19. Maximov V, Martynenko A, Hunsmann G, Tarantul V. Mitochondrial 16S rRNA gene encodes a functional peptide, a potential drug for Alzheimer's disease and target for cancer therapy. Medical Hypothese 59(6):760-673,2002

20. Guo B, Zhai,D, Cabezas E, Welsh K, Niourain S, Tatterthwait A,Reed JC.: Humanin peptide suppresses apoptosis by interfering with Bax activation. Nature,online 4 May,2003

21. Chomczynski P, Sacci N. Single-step method of RNA isolation by acid guanidium thiocyanate-phenol-chlorform extraction. Anal Biochem162:156-9,1987

22. Majima JH, Oberley TD, Fukukawa K, Mattson MP, Yen HC, Szweda LI, St. Clair DK. Prevention of mitochondrial injury by manganses superoxide dismutase reveals a primary mechanism for alkaline-induced cell death. J Biol Chem 273:8217-24,1998

23. Motoori, S., Majima, H.J., Ebara, M., Kato, H., Hirai, F., Kakinuma, S., Yamaguchi, C., Ando, K., Ozawa, T., Nagano, T., Tsujii, H., and Saisho, H.: Overexpression of mitochondrial manganese superoxide dismutase protects against radiation-induced cell death in the human hepatocellular carcinoma cell line, HLE. Cancer Res. 61:5382-5388, 2001.

24. Peng G, Taylor JD, Tchen TT. Increased mitochondrial activites in pigmented (melanized) fish cells and nucleotide sequence of mitochondrial large rRNA. Biochem Biophys Res Commun 189(1):445-9,1992

25. Baserga SJ, Linnenbach AJ, Malcolm S. Polyadenylation of a human mitochondrial ribosomal RNA transcript detected by molecular cloning. Gene 35:305-312,1985

26. Tarantul V, Nikolaev A, Hannig H. Detection of abundantly transcribed genes and gene translocation in human immunodeficiency virus-associated non-Hodgkin's lymphoma. Neoplasia 3:132-142,2001

27. Penta J, Johnson FM, Wachsman JT, Copeland WC. Mitochondrial DNA in human malignancy. Mutat Res 488:119-133,2001

28. Hashimoto Y, Niikura T, Tajima H, Yasukawa T, Sudo H, Ito Y, Kita Y, Kawasumi M, Kouyama K, Doyu M, Soube G, Koide T, Tsuji S, Lang J, Kurokawa K, Nishimoto I. A rescue factor abolishing neural cell death by a wide spectrum of familial Alzheimer's disease. PNAS 98(11):6336-6341,2001

29. Hashimoto Y, Ito Y, Niikura T. Mechanism of neuroprotection by a novel rescue factor Humanin from Swedish mutant amyloid precursor protein. Biochem Biophy Res Commun 283:460-468,2001

30. Yu W, Sanders BG, Kline K.:RRR-alpha-tocopheryl succinate-induced apoptosis of human breast cancer cells involved bax translocation to mitochondria. Cancer Res 63(109:2483-91,2003

31. Nakazawa Y, Kamijyo T, Koike K, Noda T.: ARF tumor suppressor induces mitochondria-dependent apoptosis by modulation of mitochondrial Bcl-2 family proteins. J Biol Chem ,in press, May 9, 2003

32. Muirden KD. The anemia of rheumatoid arthritis: the significance of iron deposits in the synovial membrane. Aust Ann Med 2:97-104,1970

33. Brunk UT, Terman A. The mitochondrial-lysosomal axis theory of aging: accumulation of damaged mitochondria as a result of imperfect autophagocytosis. Eur J Biochem :269(8):1996-2002,2002

34. Morris CJ, Wainwright AC, Steven MM. The nature of iron deposits in haemophilic synovitis – an immunohistochemical ultrastructural and x-ray microanalytical study. Virchows Arch [Cell Pathol] 404:75-85,1984

35. Docken WP. Pigmented villonodular synovitis: a review with illustrative case reports. Semin Arthritis Rheum 9:1-22,1979

36. Wixom RL, Prutkin L, Munro HN. Hemosiderin: nature, formation, and significance. Intl. Rev. Exper. Pathol 22:193,224,1980

37. Chamberlain MA, Petts V, Gollins E. Transport of intravenously injected ferritin across the guinea-pig synovium. Ann Rheum Dis 31:493-9,1972

38. McCord JM, Roy RS. The pathophysiology of superoxide; roles in inflammation and ischaemia. Can J Physiol Pharmacol 60:1346-52,1982

39. Halliwell B, Gutteridge JM. Oxygen toxicity, oxygen radicals, transition metals and disease. Biochem J 219:1-4,1984

40. Panduri V, Weitzman SA, Chandel N, Kamp DW. The mitochondria-regulated death pathway mediates asbestos-induced alveolar epithelial cell apoptosis. Am J Respir Cell Mol Biol ;28(2):241-8,2003

41. Gutteridge JM, Halliwell B, Treffry A, Harrison PM, Blake DR. Effect of ferritin containing

fractions with different iron loading on lipid peroxidation. Biochem J 209:557-60,1983

42. Crichton RR. Interreaction between iron methabolism and oxygen activation. In Oxygen free radicals and tissue damage. Amsterdam: Excerpta Medica:57-76,1979

43. Morris CJ, Blake DR, Wainwright AC, Steven MM. Relationship between iron deposits and tissue damage in the synovium: an ultrastructural study. Ann Rheum Dis 45:21-6,1986

Mitochondrial	
16S rRNA	30
12S rRNA	5
Homosapiens Tomoregulin mRNA	2
Homosapiens ARFGAP 1 protein mRNA	1
Mitochondrial proteolipid 68 MP homology	1
Inflammation	
β2-microglobulin mRNA	1
TGF-β mRNA	1
Fibrogenolysis	
Arg/serpin 1 plasminogen activator-inhibitor 2 mRNA	1
Homosapiens similar to serine proteinase mRNA	
Homosapiens similar to serine/arginin repetitive matrix mRNA	1
Iron metabolism	
Ferritin light chain mRNA	1
Cartilage degradation	
Homosapiens dihydropyrimidinase mRNA	1
Homosapiens osteopontin mRNA	1

Neoplastic	
L-plastin mRNA	1
Others	
Eukaryotic translation elongation factor mRNA	2
Homosapiens Nef-associated factor mRNA	1
Unknown	2
Total	68 clones

Table1. Highly expressed genes in PVNS compared with RA.

Figure Legends

Fig.1. The sequences encoded within the 16S rRNA region with poly A tail. The cDNA fragments were aligned with the 16S rRNA region of the mitochondrial gene and the correlating humanin mRNA sequence. Southern colony hybridizations repeated these sequences in a total of three rounds independently. Oblique bars show the digestion sites by Rsa I and upward diagonal bar shows the region of humanin CDS. Although there are nine types of sequences with poly A tail within this region, only the type 9 sequence was identical to the previously reported mRNA encording humanin peptide.

Fig.2. Northern blot analysis of mRNAs expressed by synovial cells from PVNS, RA and OA patients. Total RNA (168ng) was subjected to electrophoresis in a 1.0% agarose gel containing formaldehyde, transferred to nylon membrane, and probed with [^{32}P-dCTP] labeled cDNA (type 9; Table 1). Another cDNA (type 3) encoded in the 16S rRNA region was also used in Northern blotting and the expression level and size were same as those using type 9 cDNA(data not shown). Humanin genes were strongly expressed in diffuse type PVNS, but barely detected in nodular type PVNS, RA, or OA. The size of the expressed major message was ~1.6 kb and the other messages were ~1 kb, which correspond to the results of previous report by Hashimoto et al. (30)

Fig 3. The expression of genes encoded in mitochondria other than humanin genes.

Total RNA was extracted from synovial cell of 5 patients with PVNS, 3 with RA and 3 with OA and NADH dehydrogenase, ATPase 6, Cytocrome c, Cytocrome b and GAPDH mRNA levels were analyzed by semiquantitative RT-PCR. The levels of expression of these genes in PVNS were not increased in other types of arthritis, indicating that humanin gene was selectively expressed in mitochondrial genes in PVNS.

Fig 4. The expression of humanin peptide in synovial cells from diffuse type PVNS. Twenty μg of protein from synovial cell lysates were subjected to SDS-PAGE on a 5-20% gradient gel. Rabbit anti-humanin polyclonal antibody was used for Western blotting. Synthesized peptide, which was used as antigen to produce rabbit anti-humanin polyclonal antibody, was used as a standard and rabbit IgG was used as a negative control.

Fig. 5. The synovial tissue from diffuse type PVNS was fixed with 4% formaldehyde in PBS. The specimens were stained with anti-humanin antibody, followed by Alexa 488 goat anti-rabbit IgG and photographed with a fluorescent microscope(40 x). (a). Most positive cells (green) were distributed in deep layer with hemosiderin deposit. (c). Negative control of the continuous section.(b) and (d). backgrounds for a or c, respectively.

Fig. 6. The relationship between humanin peptide expression and mitochondria. Isolated hemosiderin-containing synovial cells were double-stained with anti-humanin antibody and anti

HSP 60 antibody as first antibodies, followed by goat anti-rabbit IgG and donkey anti-goat IgG as second antibodies(400 x). (a) Hemosiderin was deposited unequally throughout the cytoplasm and (d) humanin was dominantly distributed in the mitochondria around the siderosome (yellow). (b). single anti-humanin antibody staining (red). (c.) single anti-HSP 60 antibody staining (mitochondrial staining;green).

Fig. 7. Elecron micrograph of synovial cells from diffuse type PVNS. Most of the electron dense iron deposits were observed within the siderosomes. Some electron dense iron deposits were observed within mitochondria(arrows). Mitochondrial membrane debris with electron dense deposits was observed within the siderosome as an autophagosome (left arrow) (a). Some of normal mitochondria (arrows) also were scattered throughout the cytoplasm (b). (Magnification 19000 X)

Fig. 8. Electron microscopic immunohistochemistry of synovial cells from diffuse type PVNS. In some of the siderosomes, particles of colloidal-gold, were precipitated to the debris adjacent to electron dense iron (a). These results demonstrate that humanin peptide is present within the debris that are phagocytosed into the siderosome. Negative control for immunohistochemistry (b). (Magnification 29000 X)

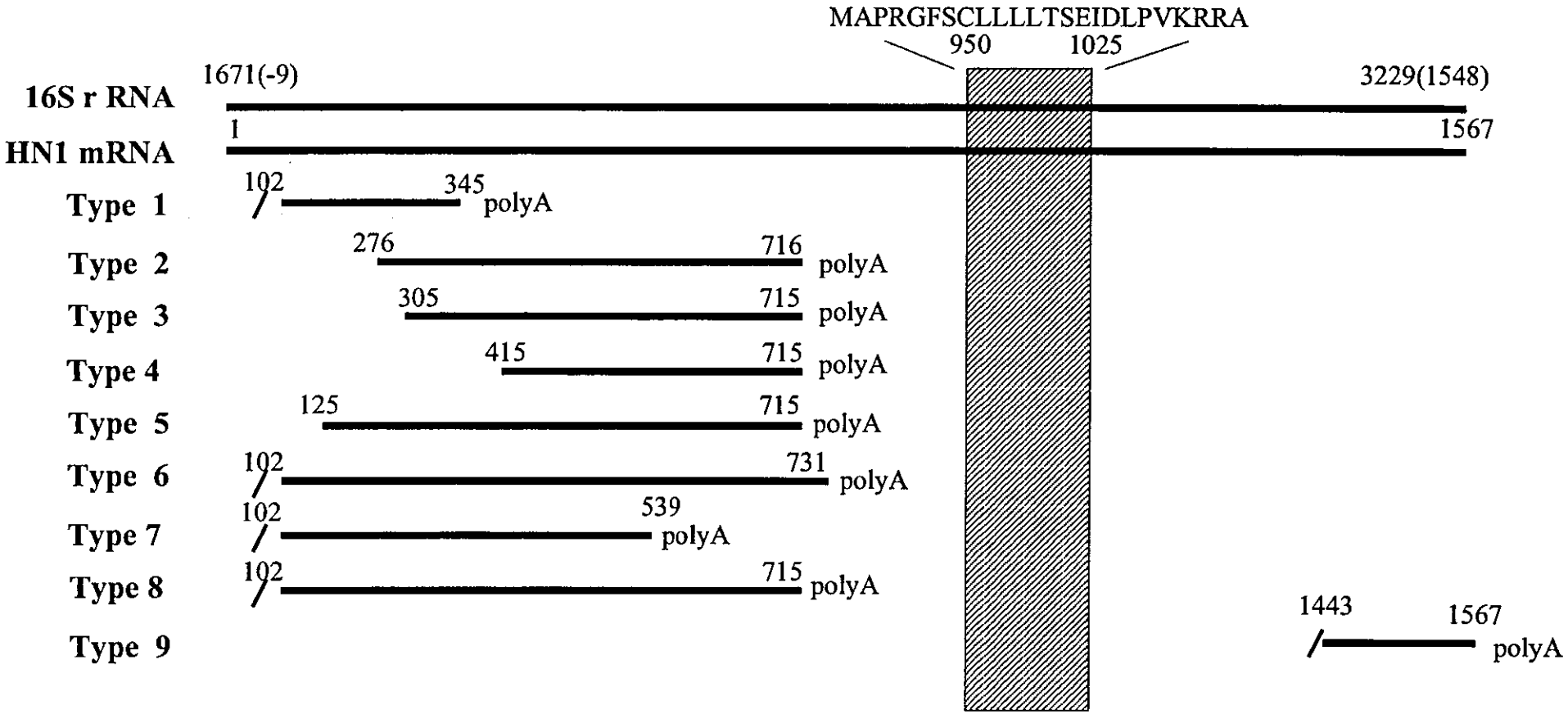

Fig.1. Kosei Ijiri